Archives of Biochemistry and Biophysics 703 (2021) 108841

Contents lists available at ScienceDirect

Archives of Biochemistry and Biophysics

journal homepage: www.elsevier.com/locate/yabbi

Leishmania major RUVBL1 has a hexameric conformation in solution and, in the presence of RUVBL2, forms a heterodimer with ATPase activity

Josielle Abrahão [a], Bárbara T. Amaro [a], Bárbara R. Peres [a], Natália G. Quel [a], Annelize Z. B. Aragão [a], Edna G.O. Morea [b], Maria Isabel N. Cano [b], Walid A. Houry [c,d], Carlos H.I. Ramos [a,*]

[a] Institute of Chemistry, University of Campinas UNICAMP, Campinas, SP, 13083-970, Brazil
[b] Department of Chemical and Biological Sciences, Biosciences Institute, Sao Paulo State University, Botucatu, SP, 18618689, Brazil
[c] Department of Biochemistry, University of Toronto, Toronto, Ontario, M5G 1M1, Canada
[d] Department of Chemistry, University of Toronto, Toronto, Ontario, M5S 3H6, Canada

ARTICLE INFO

Keywords:
Rvb
Leishmania major
AAA+ protein
DNA helicases
ATPase

ABSTRACT

ATPases belonging to the AAA+ superfamily are associated with diverse cellular activities and are mainly characterized by a nucleotide-binding domain (NBD) containing the Walker A and Walker B motifs. AAA+ proteins have a range of functions, from DNA replication to protein degradation. Rvbs, also known as RUVBLs, are AAA+ ATPases with one NBD domain and were described from human to yeast as participants of the R2TP (Rvb1-Rvb2-Tah1-Pih1) complex. Although essential for the assembly of multiprotein complexes-containing DNA and RNA, the protozoa Rvb orthologs are less studied. For the first time, this work describes the Rvbs from *Leishmania major*, one of the causative agents of Tegumentar leishmaniasis in human. Recombinant LmRUVBL1 and LmRUVBL2 his-tagged proteins were successfully purified and investigated using biophysical tools. LmRUVBL1 was able to form a well-folded elongated hexamer in solution, while LmRUVBL2 formed a large aggregate. However, the co-expression of LmRUVBL1 and LmRUVBL2 assembled the proteins into an elongated heterodimer in solution. Thermo-stability and fluorescence experiments indicated that the LmRUVBL1/2 heterodimer had ATPase activity *in vitro*. This is an interesting result because hexameric LmRUVBL1 alone had low ATPase activity. Additionally, using independent SL-RNAseq libraries, it was possible to show that both proteins are expressed in all *L. major* life stages. Specific antibodies obtained against LmRUVBLs identified the proteins in promastigotes and metacyclics cell extracts. Together, the results here presented are the first step towards the characterization of *Leishmania* Rvbs, and may contribute to the development of possible strategies to intervene against leishmaniasis, a neglected tropical disease of great medical importance.

1. Introduction

Several cellular functional processes involve protein complexes coordinated by energy-dependent conformational changes such as protein folding, proteolysis, transcription, and translation [1]. Among these protein complexes are those belonging to the AAA+ superfamily [2–4]. AAA+ proteins are adapted in a particular way to integrate a diverse number of functions [5]. These proteins are mainly characterized by the presence of a nucleotide-binding domain (NBD), which contains conserved motifs named Walker A (GX4GK [S/T]) and Walker B (hhhhDE), where X is any amino acid residue, and h is a hydrophobic residue [1,5]. These motifs are located in a region that covers about 200–250 amino acids and is named the AAA+ module [1,5].

Rvbs are AAA+ helicases and are classified as Rvb1 and Rvb2 also known as RUVBL1, Tip 49 or Pontin and RUVBL2, Tip 48 or Reptin, respectively [6]. However, other RUVBs have been also identified [6]. RUVBs play distinct roles in cell cycle progression, assembly of the telomerase complex, and the ribosomal RNA maturation complex (snoRNPs). They use the energy from ATP binding and hydrolysis to unwind DNA and RNA and assemble protein complexes [6–12].

Though RUVBL have been identified in many organisms [13–16], their paralogs in protozoa parasites that cause disease in humans and

Abbreviations: AAA, ATPases Associated with diverse cellular Activities; CD, circular dichroism; Hsp, heat shock protein; SEC-MALS, size exclusion chromatography coupled to multi-angle light scattering.

* Corresponding author.
E-mail address: cramos@unicamp.br (C.H.I. Ramos).

https://doi.org/10.1016/j.abb.2021.108841
Received 3 February 2021; Received in revised form 5 March 2021; Accepted 8 March 2021
Available online 26 March 2021

animals need to have their structure-function relationship established. This work describes the identification of putative RUVBL1 and RUVBL2 genes from the *Leishmania major*, one of the causative agents of Tegumentar leishmaniasis. This neglected tropical disease affects humans around the world. Recombinant LmRUVBL1 and LmRUVBL2, were expressed and purified alone using a bacterial system. LmRUVBL2 was produced as a large aggregate, but when co-expressed with LmRUVBL1 it generated a soluble heterodimer. LmRUVBL1/2 complexes were characterized using biophysical tools, and the results showed that they are non-globular and had ATPase activity. Additionally, it was also possible to show that both proteins are expressed in *Leishmania* promastigotes and metacyclics. Here we present a comprehensive description and characterization of RUVBLs from a protozoa parasite with great medical importance and discuss how RUVBLs can be potential targets to treat leishmaniasis.

2. Methods

2.1. Sequence analysis and cloning

The human RUVBL1 and RUVBL2 amino acid sequences (UNIPROT Q9Y265 and Q9Y230, respectively) were used to search *Leishmania major* Friedlin GeneDB (http://www.genedb.org/). Two putative ruvb-like ATPases were found, further analyzed using Blastp and named LmRUVBL1 (GeneDB ID: LmjF 34.3500) and LmRUVBL2 (GeneDB ID: LmjF 34.2610). The LmRUVBLs amino acid sequences were used to generate a multiple alignment file (Clustal Omega online tool, https://www.ebi.ac.uk/Tools/msa/clustalo/). The pre-aligned sequences were analyzed using ESPript (https://doi.org/10.1093/nar/gku316; http://espript.ibcp.fr/ESPript/cgi-bin/ESPript.cgi), and the human RUVBL1 (PDB 2C9O) was used as the template for secondary structure depiction. The encoding sequences were optimized for *E. coli* expression and synthesized by Epoch Life Science. The cDNA corresponding to the LmRUVBL1 gene was cloned between *Nde*I-*Bam*HI restriction sites in pET15b vector, which induces resistance to ampicillin. The sequence encoding LmRUVBL2 was cloned between *Bam*HI-*Eco*RI restriction sites of the pET28a + vector, which induces resistance to kanamycin, generating recombinant proteins with a His-tag at the N-terminus.

2.2. Protein expression and purification

Protein expression was performed using *E. coli* BL21 (DE3) Arctic Express transformed by heat-shock with individual plasmids, or with both plasmids for co-expression. Cells were grown in LB medium for 3 h at 30 °C, until reaching absorbance (A_{600nm}) between 0.6 and 0.8. Induction was carried out by adding 1 mM of IPTG for 24 h at 12 °C, and then cells were centrifuged at 2496×*g*, for 15 min, at 4 °C. Pellet was resuspended in lysis buffer (25 mM Tris-HCl pH 8, 500 mM NaCl, 1 mM PMSF, 30 μg/mL lysozyme, and 4U DNAse), incubated on ice for 30 min, and sonicated at 30% amplitude for 90 s.

The soluble protein fraction was injected on a nickel column (HisTrap™ HP, GE Healthcare Life Sciences) equilibrated with buffer A (25 mM Tris-HCl pH 8, 500 mM NaCl). The elution occurred in two steps with increasing imidazole concentrations (buffer A with 150 mM in the first step and 500 mM in the second). Then, size exclusion chromatography (SEC) was conducted using a Superdex 200 resin packed in an XK16/60 column (GE Healthcare Life Sciences), and sample purity was evaluated by SDS-PAGE and ImageJ (Image Processing and Analysis in Java) [17].

2.3. RUVBLs identification in L. major cell extracts and SL-seq analyses

L. major strain (MHOM/IL/1980/FRIEDLIN) was obtained from the collection of Oswaldo Cruz Institute (known as a genetically homogenous population), previously tested for Mycoplasma contamination (MycoFluor™ Mycoplasma Detection Kit; Molecular Probes). Promastigote forms were differentiated *in vitro* from amastigotes extracted from mice footpad lesions [18]. Parasites were cultivated at 26 °C in 1X M199 medium, pH 7.3, supplemented with 10% (v/v) heat-inactivated fetal calf serum, 25 mM HEPES, and 1% (v/v) antibiotic/antimycotic solution (all reagents from Cultilab) until the exponential phase and the metacyclic stage was selected from stationary phase promastigotes cultures using agglutination with peanut lectin [19].

To obtain protein extracts, parasites (~2×10^8 cells of each parasite life form) were washed twice with 1X PBS, resuspended in buffer A (20 mM Tris-HCl, pH 7.5, 1 mM EGTA, 1 mM EDTA, 15 mM NaCl, 1 mM spermidine, 0.3 mM spermine, and 1 mM DTT), frozen in liquid nitrogen for 1 min and then thawed on ice. After that, the samples were incubated with 0.5% Nonidet p-40 on ice for 30 min, centrifuged at 8000×*g* and 1X protease inhibitor cocktail (Sigma) was added to the supernatant. Western blots were developed using the polyclonal sera anti-LmRUVBL1, anti-LmRUVBL2, and *anti*-LmGAPDH used as the loading control. Anti-LmRUVBL1 and Anti-LmRUVBL2 sera were produced by RheaBiotech Inc. using the recombinant proteins described here. The secondary antibody was a goat anti-rabbit HRP-conjugated (Bio-Rad), and western blots were revealed using the enhanced chemiluminescence (ECL), according to the manufacturer's instructions (Millipore).

SL-RNA-Seq libraries (one biological replicate each) obtained from the three *L. major* life stages (amastigote, promastigote, and metacyclic), which are available as a public resource at the TriTrypDB (https://tritrypdb.org/tritrypdb/app/record/dataset/DS_8bc463a882) [20], were provided by Peter Myler's laboratory and used to analyze LmRUVBLs expression. The libraries were aligned against *L. major* Friedlin genome (TriTyrpDB v38*) with bowtie 2 (PMID: 22388286) [21] using the following parameters: very-sensitive-local-N1. Bowtie2-generated bam files were loaded into the Artemis genome browser (PMID: 22199388) [22], which allowed us to compute RPKM values for LmRUVBL1 (LmjF.34.3500) and LmRUVBL2 (LmjF.34.2610), using as a parameter an arbitrary length of 250 nt surrounding the left- or right-most non-CDS SL signal positioned 5′ upstream of each gene analyzed [23].

2.4. Spectroscopic analysis

Circular Dichroism (CD) was measured using a spectropolarimeter (JASCO J-810) and standard parameters [24]. LmRUVBLs concentrations were 5–10 μM in a 2 mm quartz cuvette, with 16 spectra accumulations at 20 °C. For thermal stability evaluation, a temperature gradient was applied to the sample, increasing 1 °C per min from 20 to 90 °C, and monitored at 222 nm.

Fluorescence spectroscopy experiments were carried out in a fluorimeter (Varian Cary Eclipse Fluorescence Spectrophotometer), with a 10 mm × 10 mm quartz cuvette. Excitation wavelength was set at 295 nm and emission was collected from 300 to 400 nm at 20 °C.

2.5. Characterization of hydrodynamic parameters

For SEC-MALS (size exclusion chromatography coupled to a multiple-angle light scattering) assays, three independent experiments were performed with 4 mg/mL of LmRUVBL1 or LmRUVBL1/2 at 20 °C using a triple-angle static light scattering detector (miniDAWN™ TREOS) and a refractive index monitor (Optilab® T-rEX) (Wyatt Technology) coupled to an AKTA FPLC system, with UV/Vis detector (GE Healthcare). Proteins were injected onto a Superdex 200 10/300 GL column (GE Healthcare) and eluted in buffer A. Raw data were processed using the ASTRA 6.0 software (Wyatt Technology) to obtain the molecular mass.

LmRUVBL1 (4 mg/mL) or LmRUVBL1/2 (2 mg/mL) samples were submitted to chromatography on a Superdex 200 10/300 GL column connected to an AKTA FPLC system (GE Life Sciences) in buffer A (described above). A calibration curve was obtained using a mix of standard monomeric proteins (thyroglobulin, ferritin, aldolase,

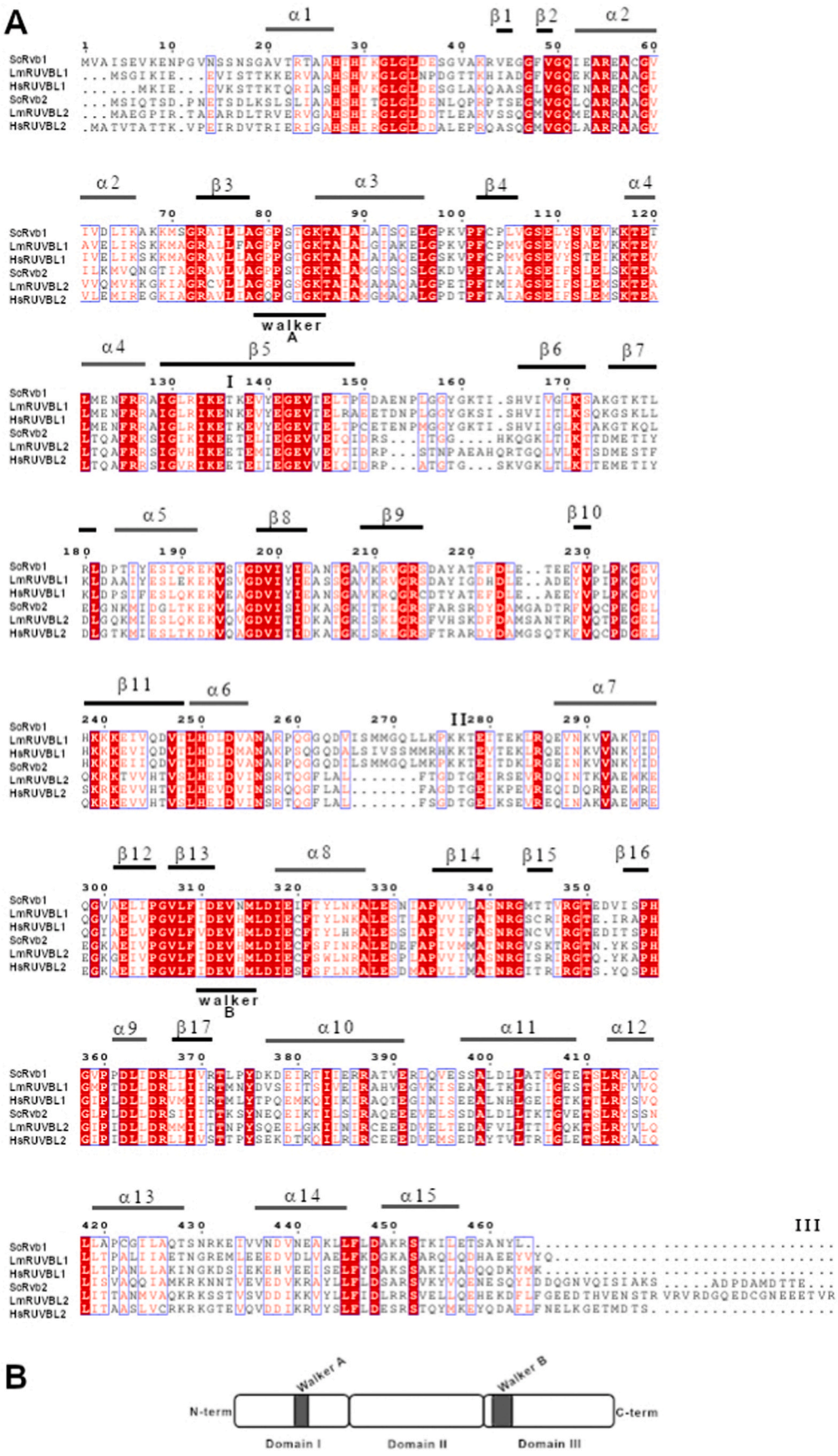

Fig. 1. LmRUVBL1 and LmRUVBL2 are highly similar to their yeast and human orthologs. A. Amino acid multiple sequence alignment indicates high similarity between *Leishmania major* RUVBL1 and RUVBL2 and their orthologs in yeast and human. Identical residues are shown in red. I, II, and III indicate domains I, II, and III, respectively, from which I and III indicate the AAA+ domain. The position of Walker A and Walker B motifs and the assigned secondary structure obtained using ESPript software (using human Rvb1 (PDB 2C9O) as the template) are depicted. Sc, *Saccharomyces cerevisiae*; Hs, *Human sapiens*; Lm, *Leishmania major*. **B.** Schematic representation of the positions of domains I-III and the Walker A and Walker B motifs (in gray) in LmRUVBL1 and LmRUVBL2. (For interpretation of the references to colour in this figure legend, the reader is referred to the Web version of this article.)

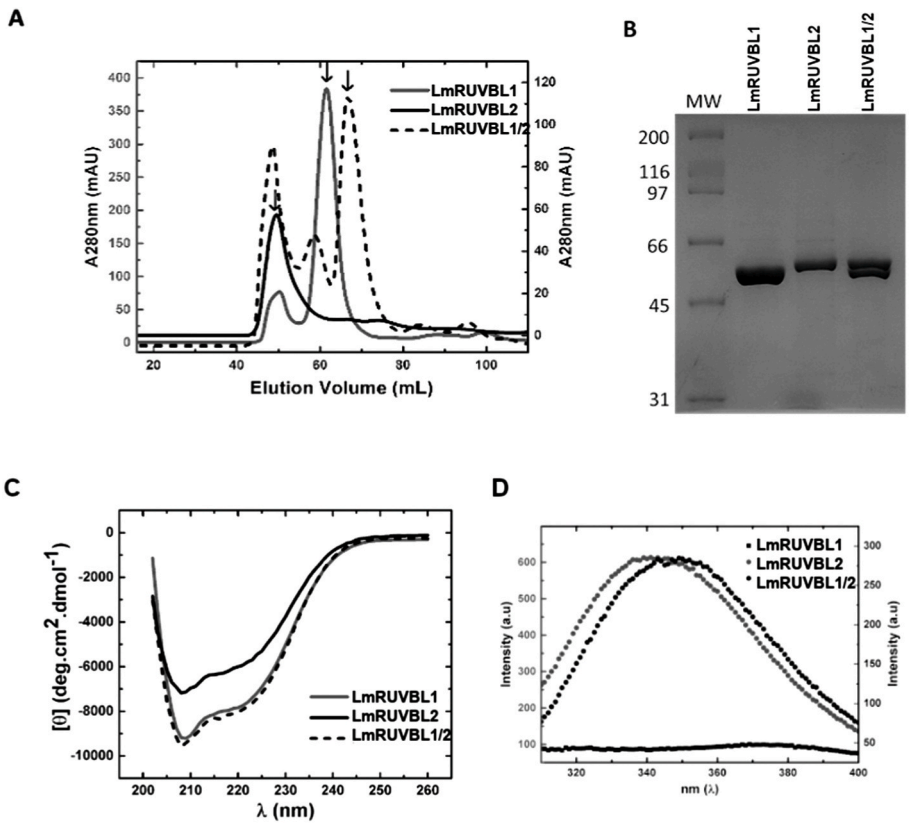

Fig. 2. LmRUVBLs purification and secondary structure analysis. **A**. SEC overlap of LmRUVBLs. LmRUVBL1 chromatogram (gray line) showed a high peak, characterized as a hexamer in solution; LmRUVBL2 eluted in the void (black line); and, after co-expression, the LmRUVBL1/2 protein was distributed in three peaks (dashed line). The third peak was used for characterization because it seemed to contain equal amounts of LmRUVBL1 and LmRUVBL2. Arrows indicate the fractions submitted to SDS-PAGE (shown in B) and further characterized (see text). **B**. SDS-PAGE 12% showed the purified proteins and their apparent molecular mass when purified individually and after co-expression (predicted mass for LmRUVBL1 = 52.35 kDa and LmRUVBL2 = 57.18 kDa). **C**. Overlap of CD spectra obtained to evaluate the secondary structure of the purified proteins, showing two minima at 208 and 222 nm, mainly indicating α-helical structure of all proteins studied. **D**. Fluorescence emission spectrum of LmRUVBL2 (gray circles) showed a maximum wavelength of 341 nm. In contrast, the spectrum of LmRUVBL1/2 (black circles) had a shift to 349 nm LmRUVBL1 (black squares) does not have Trp residues.

conalbumin and ovalbumin) (Gel Filtration Calibration Kit HMW, GE LifeSciences), with known Stokes or hydrodynamic radius (R_s). The R_s of each standard protein was plotted against (-log Kav) ^{½} and adjusted by linear fitting analysis.

Dynamic light scattering experiments were carried out using a Malvern Zetasizer Nano ZS 90 (Model 3690) instrument equipped with a 633 nm laser, in a polystyrene cell. Samples of LmRUVBL1 (10–300 μM) and LmRUVBL1/2 (70 μM) in buffer A had their light scattering intensity monitored at 20 °C, 20 repetitions each measurement.

2.6. ATPase activity assessment

LmRUVBLs ATPase activity was assessed using the ATP/NADH coupled assay [25]. The reactions were carried out in 96-well plates in a buffer containing 25 mM Tris-HCl, 500 mM NaCl, 8 mM $MgCl_2$, pH 8.0 mixed with 3 mM phosphoenolpyruvate, 0.3 mM NADH, 40 U/mL pyruvate kinase and 58 U/mL lactate dehydrogenase. ATPase reaction was started by the addition of ATP (pH 7.0) at a final concentration of 5 mM. Readings were taken at 340 nm in a Biotek Synergy HT® plate reader at 37 °C for 90 min. LmRUVBLs concentration was 5 μM.

3. Results and discussion

3.1. Leishmania RUVBLs have a high identity with their yeast and human orthologs

To identify and characterize two important AAA+ ATPases in *L. major*, GeneDB was searched using BLASTp to identify RUVB-like ATPases using the human RUVBL1 (TIP48 or Pontin) and RUVBL2 (TIP49 or Reptin) as queries. Two putative RUVBL genes were identified in *L. major* genome with IDs: LmjF 34.3500 and LmjF 34.2610. Orthologs of RUVBL1 and RUVBL2 have been identified in different protozoa, such as *Plasmodium falciparum* and *L. donavani*, as helicases that interact with DNA/RNA and proteins complexes [26–29]. Despite the functional information generated by these studies, there is a lack of structural information about the protozoa's RUVBLs. On the other hand, yeast and human RUVBLs [11,12,30,31] are much better studied and share about 60–70% sequence identity with *L. major* RUVBLs (Fig. 1A), named here as LmRUVBL1 and LmRUVBL2. LmRUVBL1 is 458 residues long (50.1 kDa), while LmRUVBL2 is 483 residues long (53.6 KDa), which are identical to the RUVBLs described in *L. donovani* [29]. The secondary structure assigned by ESPript software, using the crystallographic structure of human RUVBL1 (PDB 2C9O) was used as the template, showing that the *L. major* RUVBL proteins have the same domain organization as the human and yeast Rvbs (Fig. 1A), including the essential motifs, Walker A and Walker B motifs involved in ATPase activity (Fig. 1B).

3.2. Purification and folded states of LmRUVBLs

The cDNA from the putative genes were cloned, and the recombinant proteins were expressed. LmRUVBL1 and LmRUVBL2 were obtained alone or co-expressed and purified using nickel affinity chromatography (Supplementary Figure S1) followed by SEC (Fig. 2A). Protein purity was determined as >95% by ImageJ software. Initially, we investigated the oligomeric state of the purified proteins by SEC (Fig. 2A).

The SEC profile for LmRUVBL1 (Fig. 2A) demonstrated two peaks, a minor one that eluted in the void and likely represented large aggregates, and a major one (marked by an arrow) that consisted of a soluble hexamer and was more than 95% pure (Fig. 2B). On the other hand, the LmRUVBL2 SEC profile (Fig. 2A) exhibited only one peak that eluted in the void and was aggregated (marked by an arrow; see below) but with more than 95% purity (Fig. 2B). Additionally, the co-expression of both LmRUVBL1 and LmRUVBL2, here designated as LmRUVBL1/2, had a SEC profile with three peaks (Fig. 2A). One at the void corresponding to large aggregates, a second overlapping peak that was too diluted to allow further experimentation and a major one (marked by an arrow) that consisted of a soluble heterodimer and was more than 95% pure

Table 1
LmRUVBLs characteristics.

Protein	Major oligomeric state (investigated by SEC)	Secondary structure stable up to (investigated by CD)	Tryptophan maximum wavelength (investigated by emission fluorescence)
LmRUVBL1	Hexamer	45 °C	–
LmRUVBL2	Large aggregate	55 °C	341 nm
LmRUVBL1/2	Heterodimer	70 °C	349 nm

(Fig. 2B). Due to these characteristics, the study started only with the peaks identified by an arrow in Fig. 2A (see Table 1) and only the soluble hexameric LmRUVBL1 and heterodimeric LmRUVBL1/2, were further characterized (see below). Additionally, the samples identified by the arrows behaved as single species (see below). Indeed, the solubilization of RUVBLs from parasites is challenging. For instance, both RUVBL1 [25] and RUVBL3, an analog of RUVBL2, [27] from *P. falciparum* required the assistance of chaperones to increase their solubility.

The secondary structure of each protein was evaluated by CD, and all three spectra showed two minima at 208 and 222 nm (Fig. 2C), indicating that the proteins were mainly α-helical. The percentage of α-helix in LmRUVBL1 was calculated as ~27% and in LmRUVBL2 as ~22%. The crystallographic structure of human RUVBL1 demonstrated that the monomer has 14 α-helices and 16-β sheets [12] which is in good agreement with the secondary structure prediction shown in Fig. 1A. Additionally, the CD spectrum of LmRUVBL1/2 had more signal than expected for the sum of LmRUVBL1 and LmRUVBL2 spectra, which was intermediate of those of the proteins alone (Fig. 2C). These results indicate that LmRUVBL2 had an increase in secondary structure in the presence of LmRUVBL1 and also increased its solubility as confirmed by further investigation (see below). The secondary structure of the complex was more stable when exposed to increasing temperatures as shown by CD. LmRUVBL1 maintained the CD signal at 222 nm up to 45 °C, LmRUVBL2 up to 55 °C and LmRUVBL1/2 up to 70 °C (Table 1).

It is important to note that while LmRUVBL1 does not have Trp residues in its sequence, LmRUVBL2 has two Trp residues (see Fig. 1A). When purified alone, the Trp of LmRUVBL2 emitted with maximum wavelength at 341 nm, but shifted the emission to 349 nm when co-expressed with LmRUVBL1 (Fig. 2D and Table 1). This result indicates that the co-expression with LmRUVBL1 changed the conformation of LmRUVBL2 because tryptophan (Trp) fluorescence is sensitive to the polarity of its environment as the wavelength of maximum emission has a red-shift in a polar environment [32].

It is noteworthy that an increase in stability was also observed for the RUVBLs from the fungus *Chaetomium thermophilum*, whereby the individual proteins had lower stability than the dodecameric complex [33]. Unfortunately, subsequent experiments using LmRUVBL2 alone were not possible since only aggregated protein species were detected (Fig. 2A). Nevertheless, our results reinforced the hypothesis that the presence of LmRUVBL1 stabilizes LmRUVBL2 in the conditions studied here.

3.3. RUVBLs were identified in L. major cell extracts

The next step involved verifying the endogenous expression of the RUVBLs coding genes by *L. major* cells. For that, independent Splice Leader (SL) RNA-Seq (SL-RNA-Seq) libraries analyses were used, and it was possible to confirm that both LmRUVBL1 and LmRUVBL2 were expressed in all parasite's developmental stages (Supplementary Table S1). In *Leishmania* sp., as in other trypanosomatids, mRNAs are processed by *trans*-splicing, by the addition of a 39 nt long SL (splice leader) sequence containing a 5′capped tri-methyl guanosine, coupled with the addition of a poly-A tail at the 3′ end of the upstream gene in the polycistron [34]. SL is a conserved marker of RNA maturation in

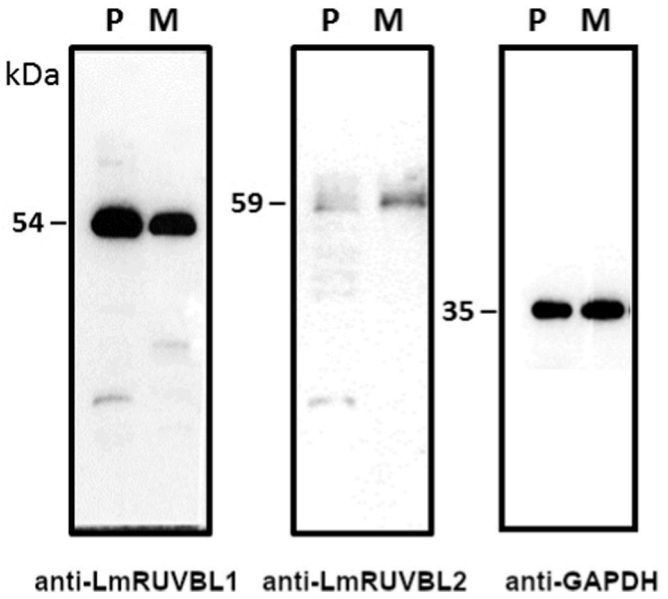

Fig. 3. RUVBLs were identified in *L. major* promastigotes and metacyclics cell extracts of. Total extracts (60 μg/well) obtained from promastigote (P) or metacyclic (M) forms were fractionated in 12% SDS-PAGE, transferred to nitrocellulose membranes and revealed using ECL after WB with specific polyclonal antibodies against LmRUVBL1 (1:3000), LmRUVBL2 (1:5000), and LmGAPDH (1:2000) used as the loading control.

trypanosomatids and the SL-RNA-seq libraries are sequenced based on the presence of the SL sequence at the 5′ end of each transcript [19]. The RPKM (Supplementary Table S1) represents the average analyses of two biological replicates of each library.

The difference in mRNA measurements between developmental stages is probably due to unknown regulatory elements at the LmRUVBLs 3′UTR [35–37]. As a matter of fact, regulatory elements would positively control mRNA expression and stabilization only in promastigotes, justifying the results obtained in the SL-seq libraries. Genetic reprogramming during parasite development induces differences in promastigotes and balanced amastigotes and metacyclics in respect to gene expression profiles [38]. Additionally, mRNA abundance differences during parasite development were widely described for *Leishmania* sp. [see, for instance: [39,40]].

Extracts from *L. major* were further used in Western blot experiments (Fig. 3) using polyclonal antibodies produced from the recombinant proteins (see Supplementary Figure S2). In these experiments, *anti*-LmGAPDH was used as the loading control. The analysis of Fig. 3 clearly shows the presence of proteins with molecular masses (MM) similar to promastigote and metacyclic LmRUVBL1 and LmRUVBL2. It was possible to identify few differences in protein abundance among parasite life stages, compared to the proteins used as the loading controls. In this context, it is important to point that the regulation of both mRNA and protein levels dynamically alters in *Leishmania* because they depend on both the protein function and the environmental circumstances that the parasite encounters during adaptation to live and survive in different hosts [41].

3.4. Oligomeric state and conformation of LmRUVBLs

First, SEC-MALS was used to measure the molecular masses (MM) of the LmRUVBLs, which were 333.0 ± 12.0 kDa for LmRUVBL1 and 120.1 ± 3.2 kDa for LmRUVBL1/2 (Fig. 4A). Since the theoretical MM of LmRUVBL1 monomer is 52.35 kDa, the protein was a hexamer in solution. As a matter of fact, several helicases oligomerize as they are usually composed of more than one subunit [12,13,42–45]. The crystallographic structure of the human RUVBL1 protein showed a

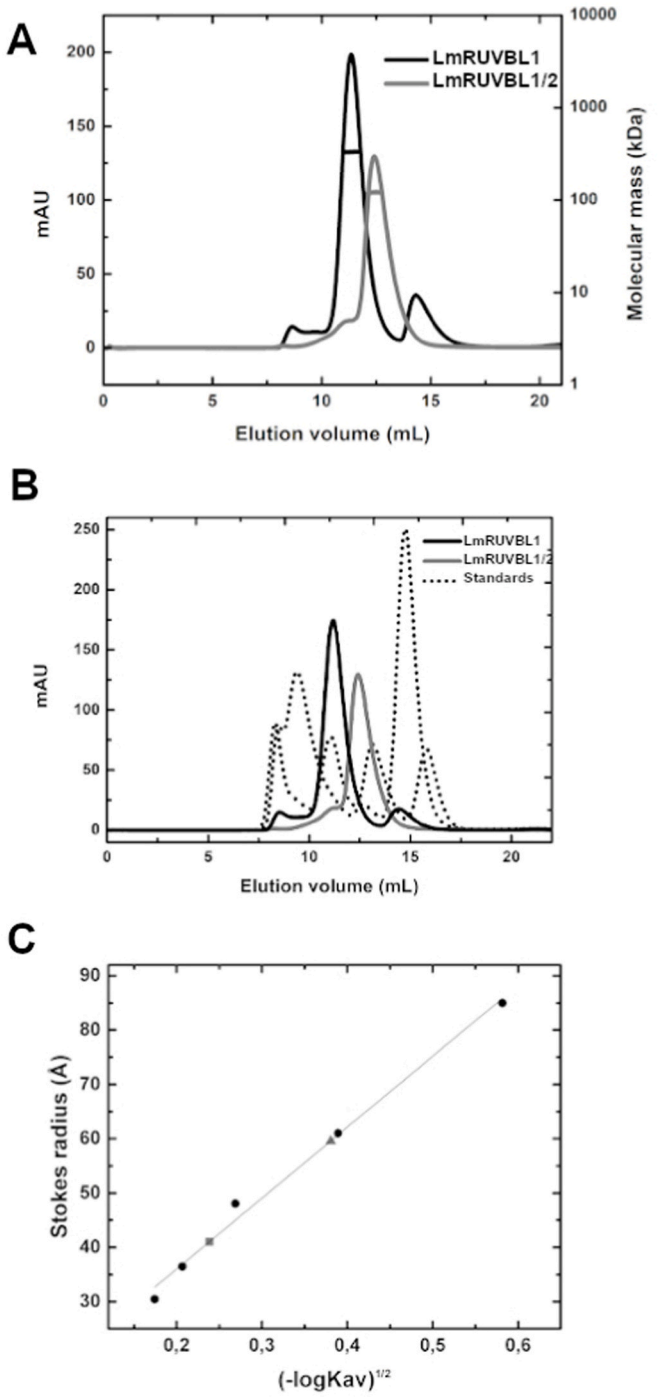

Fig. 4. Characterization of LmRUVBLs oligomeric state. A. SEC-MALS of LmRUVBL1 (black line) and LmRUVBL1/2 (gray line). Proteins were injected at 4 and 2 mg/mL, respectively, in 25 mM Tris-HCl/500 mM NaCl (pH 8) buffer. All data were analyzed with the ASTRA program (Wyatt Technologies), and the molecular mass of LmRUVBL1 was 333 ± 12 kDa, and LmRUVBL1/2 was 120.1 ± 3.2 kDa. **B.** Chromatogram of standard proteins (dotted line), LmRUVBL1 (black line) and LmRUVBL1/2 (gray line). **C.** Calibration curve as a function of R_s indicating that LmRUVBL1 (gray triangle) had an R_s of 59.0 ± 1.0 Å and LmRUVBL1/2 (gray square) had an R_s of 41.0 ± 1.0 Å.

hexameric ring conformation [12], corroborating the *L. major* ortholog results. The human RUVBL2 is also capable of oligomerization to form a homohexamer in solution [46]. However, we could not get this conformation in the conditions used in this work as LmRUVBL2 was purified as a large aggregate.

Table 2
Measured *versus* predicted hydrodynamic parameters.

	Parameter/ technique	Measured	Predicted
LmRUVBL1 (homohexamer)	R_s (Å)/aSEC	59.9 ± 1.0	20.8[a]
	D (cm^2/s)/DLS	2.4 ± 0.3 × 10^{-7}	10.4[a]
	MM (kDa)/SEC-MALS	332.8 ± 12.0	314.1[b]
LmRUVBL1/2 (heterodimer)	R_s (Å)/aSEC	41.1 ± 1.0 Å	32.1[a]
	D (cm^2/s)/DLS	2.4 ± 0.5 × 10^{-7}	6.6 × 10^{-7}[a]
	MM (kDa)/SEC-MALS	120.1 ± 3.2	109.6[b]

[a] For a non-hydrated sphere with the same molecular mass of the respective oligomer.
[b] From sequence.

Nonetheless, the theoretical MM for a heterodimer is 109.53 kDa (combined LmRUVBL1 and LmRUVBL2 monomers), confirming that the molecular mass obtained by SEC-MALS for LmRUVBL1/2, 120.1 ± 3.2 kDa, corresponds to a heterodimer in solution. It has been reported [47] that yeast Rvbs form a heterodimer in solution when the His-tag is present, as observed here, but form heterohexamers in the absence of His-tag. Unfortunately, several strategies were tried (data not shown) to remove the His-tag from LmRUVBLs but were unsuccessful. Other studies observed differences in oligomerization when only RUVBL1, or RUVBL2, or both proteins had the His-tag. When only one protein had the tag, hexamers, and dodecamers were found in solution. However, when both RUVBLs are tag-less, they formed dodecamers [42,43,47] predominantly. Additionally, an assembly pathway to form dodecamer may involve the formation of monomers, dimers, trimers, and hexamers as intermediates [48], showing that RUVBLs can have more than one oligomerization state in solution. In the conditions studied here, the hexameric state of LmRUVBL1 and the heterodimeric state of LmRUVBL1/2 predominated.

Then, hydrodynamic parameters of the LmRUVBLs were determined to get information on the global conformation of these proteins. Analysis by SEC required standard proteins to be used to generate a calibration curve by plotting Kav values $(-\log Kav)^{1/2}$, which is the distribution coefficient obtained from the elution volume of each protein, as a function of R_s (Stokes or hydrodynamic radius; Table 2 and Fig. 4B and C). Calibration curve analysis indicated that LmRUVBL1 had an R_s of 59.0 ± 1.0 Å and LmRUVBL1/2 had an R_s of 41.0 ± 1.0 Å (Table 2 and Fig. 4B).

Following that, samples were prepared, and 20 independent measurements were made using the DLS equipment. The measured diffusion coefficient (D) was 2.4 ± 0.5 × 10^{-7} cm^2/s for LmRUVBL1 and 2.4 ± 0.3 × 10^{-7} cm^2/s for LmRUVBL1/2 (Table 2). Because it is possible to predict the R_s and D values for non-hydrated spheres of known MM (see Ref. [49] for review), one can compare the predicted values with those measured experimentally and evaluate whether or not the protein conformation is globular. The predicted and measured R_s and D values are shown in Table 2, and they differ, for both complexes, much more than expected considering only hydration. Therefore, both the hexameric LmRUVBL1 and the heterodimeric LmRUVBL1/2 had non-globular conformations, being likely elongated. These results are in good agreement with what is currently known about the structure of RUVBLs showing that the monomeric unit is elongated, and that oligomers tend to be single or double-ring-shaped (for structural comparisons, see [44,50]).

3.5. The heterodimer has ATPase activity in vitro

LmRUVBLs are members of the AAA+ protein superfamily and probably are active ATPases. Therefore, their function as ATPases was tested. The reactions were evaluated as a function of time. The ATP

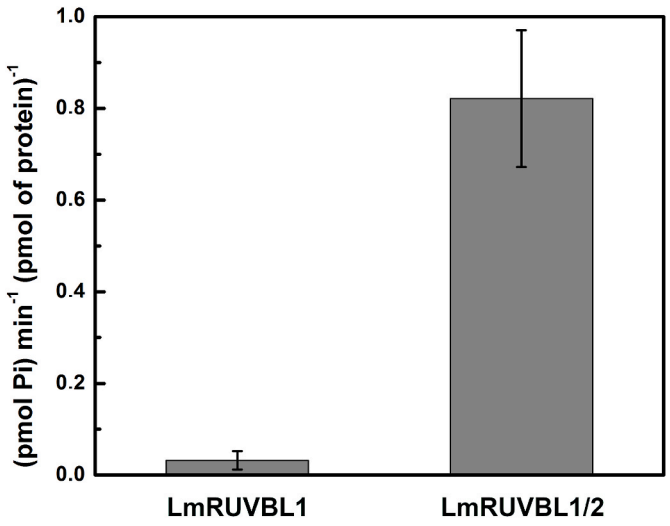

Fig. 5. Hydrolysis rate. The oxidation of NADH monitored ATP hydrolysis rate as a function of time. LmRUVBL1 has low ATPase activity while LmRUVBL1/2 was about 40x more active.

hydrolysis rate was calculated as a function of inorganic phosphate (in pmol) released per minute for pmol of protein monomer (Fig. 5). The ATPase activity of hexameric LmRUVBL1 was very low compared with that of LmRUVBL1/2, which was approximately 40 times higher. These results add important insights about the RUVBLs from *Leishmania* as they behave similarly to human RUVBLs. Human RUVBL1 has little activity *in vitro* [12] but in the presence of RUVBL2 the complex has high ATPase activity [30].

On the other hand, yeast Rvbs seem to behave differently, as Rvb2 has little activity [13]. Nonetheless, the yeast Rvb1/2 complex has high ATPase activity [13]. Actually, when other eukaryotic organisms are considered, there are isolated AAA+ proteins with low activity, but the activity usually increases when heterocomplexes are formed [51]. These observations reinforce the claim that the study of orthologs increases the general understanding of the relationship between structure and function for these proteins.

4. Conclusion

RUVBLs belong to the AAA+ family of ATPases that play essential cellular functions such as chromatin remodeling, DNA repair, ribosomal RNA processing, and assembly of telomerase complexes. This work describes the cloning and purification of RUVBL1 and RUVBL2 from *L. major*, named LmRUVBL1 and LmRUVBL2, respectively. The proteins were found to be expressed in both promastigote and metacyclic developmental stages of the parasite, indicating that the study of these proteins is important for the biological understanding of this organism, hopefully by generating knowledge that can be used in therapeutic strategies.

Protein expression and purification confirmed that the DNA sequences here investigated were translated into stable polypeptides. However, protozoa proteins are sometimes hard to purify in sufficient amounts and solubility to allow proper investigation. The hexameric form of his-tagged LmRUVBL1 and the heterodimeric estate of LmRUVBL1/2 were soluble and were investigated by biophysical tools. Both forms were stable at temperatures higher than that of the environments in which the parasite lives, and had an elongated shape as expected for the Rvbs. While LmRUVBL1 showed low ATPase activity in the conditions tested, LmRUVBL1/2 had a much higher ATPase activity. Nonetheless, because removal of the his-tag was not possible our work may represent the characterization of only one of the multiple oligomerization states that LmRUVBLs are capable to access in solution [42,43,47,48].

Our work sets the stage for future studies to be carried out to understand the structure and cellular function of these conserved ATPases in parasites.

Authorship contribution

J.A, B.T.A., B.R.P., N.G.Q., A. Z.B.A., E.G.O.M.: Data collection, analysis, and interpretation. W.A.H., M.I.N.C., C.H.I.R.: Data analysis and interpretation. C.H.I.R.: designed the work. All authors: drafted and critically reviewed the article.

Declaration of competing interest

The authors declare no competing interests.

Acknowledgments

This work was supported by FAPESP (2012/50161-8; 2017/26131-5), CAPES (99999.004913/2015-09; Brazil), Foreign Affairs, Trade, and Development Canada (DFATD) grant. CHIR and MINC have a research fellowship from CNPq. JA (2013/10939-2; 2015/13521-4) NGQ (2014/25967-4) and EGOM (2019/11496-3) received a fellowship from FAPESP. WAH is supported by a CIHR Project grant (PJT-173491).

Appendix A. Supplementary data

Supplementary data to this article can be found online at https://doi.org/10.1016/j.abb.2021.108841.

References

[1] A.F. Neuwald, L. Aravind, J.L. Spouge, E.V. Koonin, AAA+: a class of chaperone-like ATPases associated with the assembly, operation, and disassembly of protein complexes, Genome Res. 9 (1999) 27–43, https://doi.org/10.1101/gr.9.1.27.
[2] P.I. Hanson, S.W. Whiteheart, AAA+ proteins: have engine, will work, Mol. Cell Biol. 6 (2005) 519–529, https://doi.org/10.1038/nrm1684.
[3] A.N. Lupas, J. Martin, AAA proteins, Curr. Opin. Struct. Biol. 12 (2002) 746–753, https://doi.org/10.1016/s0959-440x(02)00388-3.
[4] L.M. Iyer, D.D. Leipe, E.V. Koonin, L. Aravind, Evolutionary history and higher order classification of AAA+ ATPases, J. Struct. Biol. 146 (2004) 11–31, https://doi.org/10.1016/j.jsb.2003.10.010.
[5] J. Snider, W.A. Houry, AAA+ proteins: diversity in function, similarity in structure, Biochem. Soc. Trans. 36 (2008) 72–77, https://doi.org/10.1042/BST0360072.
[6] Y. Wu, Unwinding and rewinding: double faces of helicase? J. Nucleic Acids (2012) 140601, https://doi.org/10.1155/2012/140601.
[7] W.A. Houry, E. Bertrand, B. Coulombe, The PAQosome, an r2tp-based chaperone for quaternary structure formation, Trends Biochem. Sci. 43 (2018) 4–9, https://doi.org/10.1016/j.tibs.2017.11.001.
[8] T. Ikura, V. V Ogryzko, M. Grigoriev, R. Groisman, J. Wang, M. Horikoshi, R. Scully, J. Qin, Y. Nakatani, Involvement of the TIP60 histone acetylase complex in DNA repair and apoptosis, Cell 102 (2000) 463–473, https://doi.org/10.1016/S0092-8674(00)00051-9.
[9] Y. Kakihara, T. Makhnevych, L. Zhao, W. Tang, W.A. Houry, Nutritional status modulates box C/D snoRNP biogenesis by regulated subcellular relocalization of the R2TP complex, Genome Biol. 15 (2014) 1–20, https://doi.org/10.1186/s13059-014-0404-4.
[10] N. Nano, W.A. Houry, Chaperone-like activity of the AAA+ proteins Rvb1 and Rvb2 in the assembly of various complexes, Philos. Trans. R. Soc. Lond. B Biol. Sci. 368 (2013) 20110399, https://doi.org/10.1098/rstb.2011.0399.
[11] S. Gorynia, T.M. Bandeiras, F.G. Pinho, C.E. McVey, C. Vonrhein, A. Round, D. I. Svergun, P. Donner, P.M. Matias, M.A. Carrondo, Structural and functional insights into a dodecameric molecular machine - the RuvBL1/RuvBL2 complex, J. Struct. Biol. 176 (2011) 279–291, https://doi.org/10.1016/j.jsb.2011.09.001.
[12] P.M. Matias, S. Gorynia, P. Donner, M.A. Carrondo, Crystal structure of the human AAA + protein RuvBL1, J. Biol. Chem. 281 (2006) 38918–38929, https://doi.org/10.1074/jbc.M605625200.
[13] A. Gribun, K.L.Y. Cheung, J. Huen, J. Ortega, W.A. Houry, Yeast Rvb1 and Rvb2 are ATP-dependent DNA helicases that form a heterohexameric complex, J. Mol. Biol. 376 (2008) 1320–1333, https://doi.org/10.1016/j.jmb.2007.12.049.
[14] O. Huber, L. Menard, V. Haurie, A. Nicou, D. Taras, J. Rosenbaum, Pontin, Reptin, Two related ATPases with multiple roles in cancer, Canc. Res. 68 (2008) 6873–6876, https://doi.org/10.1158/0008-5472.CAN-08-0547.
[15] H. Guo, X.-Y. Zhanga, J. Peng, Y. Huang, Y. Yang, Y. Liu, X.-X. Guo, Q. Hao, S. An, T.-R. Xu, RUVBL1, a novel C-RAF-binding protein, activates the RAF/MEK/ERK

pathway to promote lung cancer tumorigenesis, Biochem. Biophys. Res. Commun. 498 (2018) 932–939, https://doi.org/10.1016/j.bbrc.2018.03.084.
[16] S.K. Saifi, N. Passricha, R. Tuteja, N. Tuteja, An overview of AAA+ superfamily proteins associated helicases, in: Helicases from All Domains Life, 2019, pp. 247–264, https://doi.org/10.1016/B978-0-12-814685-9.00015-4.
[17] C.T. Rueden, J. Schindelin, M.C. Hiner, B.E. DeZonia, A.E. Walter, E.T. Arena, K. W. Eliceiri, ImageJ 2: ImageJ for the next generation of scientific image data, BMC Bioinf. 18 (2017) 529, https://doi.org/10.1186/s12859-017-1934-z.
[18] C.L. Barbiéri, A.I. Doine, E. Freymuller, Lysosomal depletion in macrophages from spleen and foot lesions of *Leishmania*-infected hamster, Exp. Parasitol. 71 (1990) 718–728, https://doi.org/10.1016/0014-4894(90)90024-7.
[19] R. da Silva, D.L. Sacks, Metacyclogenesis is a major determinant of *Leishmania* promastigote virulence and attenuation, Infect. Immun. 55 (1987) 2802–2806, https://doi.org/10.1128/iai.55.11.2802-2806.1987.
[20] B. Cuypers, M.A. Domagalska, P. Meysman, G. de Muylder, M. Vanaerschot, H. Imamura, F. Dumetz, T.W. Verdonckt, P.J. Myler, G. Ramasamy, K. Laukens, J.-C. Dujardin, Multiplexed spliced-708 leader sequencing: a high-throughput, selective method for RNA-seq in trypanosomatids, Sci. Rep. 7 (2017) 3725, https://doi.org/10.1038/s41598-017-03987-0.
[21] B. Langmead, S.L. Salzberg, Fast gapped-read alignment with Bowtie 2, Nat. Methods 9 (2012) 357–359, https://doi.org/10.1038/nmeth.1923.
[22] T. Carver, S.R. Harris, M. Berriman, J. Parkhill, J.A. McQuillan, Artemis: an integrated platform for visualization and analysis of high-throughput sequence-based experimental data, Bioinformatics 28 (2012) 464–469, https://doi.org/10.1093/bioinformatics/btr703.
[23] A. Mortazavi, B.A. Williams, K. McCue, L. Schaeffer, B. Wold, Mapping and quantifying mammalian transcriptomes by RNA-Seq, Nat. Methods 5 (2008) 621–628, https://doi.org/10.1038/nmeth.1226.
[24] D.H.A. Correa, C.H.I. Ramos, The use of circular dichroism spectroscopy to study protein folding, form and function, Afr. J. Biochem. Res. 3 (2009) 164–173. https://www.researchgate.net/profile/Daniel_Correa5/publication/228351774_The_use_of_circular_dichroism_spectroscopy_to_study_protein_folding_form_and_function/links/0c96051a39700a319c000000.pdf.
[25] J.G. Nørby, Coupled assay of Na+,K+-ATPase activity, Methods Enzymol. 156 (1988) 116–119. http://www.ncbi.nlm.nih.gov/pubmed/2835597.
[26] M. Ahmad, S. Singh, F. Afrin, R. Tuteja, Novel RuvB nuclear ATPase is specific to intraerythrocytic mitosis during schizogony of Plasmodium falciparum, Mol. Biochem. Parasitol. 185 (2012) 58–65, https://doi.org/10.1016/j.molbiopara.2012.06.002.
[27] M. Ahmad, R. Tuteja, *Plasmodium falciparum* RuvB2 translocates in 5'-3' direction, relocalizes during schizont stage and its enzymatic activities are up regulated by RuvB3 of the same complex, Biochim. Biophys. Acta Protein Proteonomics 1834 (2013) 2795–2811, https://doi.org/10.1016/j.bbapap.2013.
[28] M. Ahmad, R. Tuteja, *Plasmodium falciparum* RuvB1 is an active DNA helicase and translocates in the 5'-3' direction, Gene 515 (2013) 99–109, https://doi.org/10.1016/j.gene.2012.11.020.
[29] M. Ahmad, F. Afrin, R. Tuteja, Identification of R2TP complex of *Leishmania donovani* and *Plasmodium falciparum* using genome wide in-silico analysis, Commun. Integr. Biol. 6 (2013) 1–10, https://doi.org/10.4161/cib.26005.
[30] T. Puri, P. Wendler, B. Sigala, H. Saibil, I.R. Tsaneva, Dodecameric structure and ATPase activity of the human TIP48/TIP49 complex, J. Mol. Biol. 366 (2007) 179–192, https://doi.org/10.1016/j.jmb.2006.11.030.
[31] J. Rosenbaum, S.H. Baek, A. Dutta, W.A. Houry, O. Huber, T.R. Hupp, P.M. Matias, The emergence of the conserved AAA+ ATPases Pontin and Reptin on the signaling landscape, Sci. Signal. 6 (2013), https://doi.org/10.1126/scisignal.2003906.
[32] M.R. Eftink, Fluorescence techniques for studying protein structure, Methods Biochem. Anal. (1991) 127–205, https://doi.org/10.1002/9780470110560.ch3.
[33] N. Silva-Martin, M.I. Daudén, S. Glatt, iklas A. Hoffmann, P. Kastritis, P. Bork, M. Beck, C.W. Müller, The combination of X-ray crystallography and cryo-electron microscopy provides insight into the overall architecture of the dodecameric rvb1/rvb2 complex, PloS One 11 (2016) 1–18, https://doi.org/10.1371/journal.pone.0146457.
[34] S.M.R. Teixeira, B.M. Valente, Mechanisms controlling gene expression in trypanosomatids, in: Front. Parasitol, 2017, pp. 261–290.
[35] K.K. Mishra, T.R. Holzer, L.L. Moore, J.H. LeBowitz, A negative regulatory element controls mRNA abundance of the *Leishmania mexicana* paraflagellar rod gene PFR2, Eukaryot. Cell 2 (2003) 1009–1017, https://doi.org/10.1128/EC.2.5.1009-1017.2003.
[36] A. Rochette, F. McNicoll, J. Girard, M. Breton, E. Leblancc, M.G. Bergeron, B. Papadopoulou, Characterization and developmental gene regulation of a large gene family encoding amastin surface proteins in *Leishmania* spp, Mol. Biochem. Parasitol. 140 (2005) 205–220, https://doi.org/10.1016/j.molbiopara.2005.01.006.
[37] E.J.R. Vasconcelos, M.C. Terrão, J.C. Ruiz, R.Z.N. Vêncio, A.K. Cruz, In silico identification of conserved intercoding sequences in Leishmania genomes: unraveling putative cis-regulatory elements, Mol. Biochem. Parasitol. 183 (2012) 140–150, https://doi.org/10.1016/j.molbiopara.2012.02.009.
[38] E. Inbar, V.K. Hughitt, L.A.L. Dillon, K. Ghosh, N.M. El-Sayed, D.L. Sacks, The transcriptome of *Leishmania major* developmental stages in their natural sand fly vector, mBio (2017), https://doi.org/10.1128/mBio.00029-17 e00029-17.
[39] N.S. Akopyants, R.S. Matlib, E.N. Bukanova, M.R. Smeds, B.H. Brownstein, G. D. Stormo, S.M. Beverley, Expression profiling using random genomic DNA microarrays identifies differentially expressed genes associated with three major developmental stages of the protozoan parasite *Leishmania major*, Mol. Biochem. Parasitol. 136 (2004) 71–86, https://doi.org/10.1016/j.molbiopara.2004.03.002.
[40] A. Saxena, T. Lahav, N. Holland, G. Aggarwal, A. Anupama, Y. Huang, H. Volpin, P. J. Myler, D. Zilberstein, Analysis of the *Leishmania donovani* transcriptome reveals an ordered progression of transient and permanent changes in gene expression during differentiation, Mol. Biochem. Parasitol. 152 (2007) 53–65, https://doi.org/10.1016/j.mib.2007.10.001.
[41] P.J. Alcolea, A. Alonso, R. Molina, M. Jiménez, P.J. Myler, V. Larraga, Functional genomics in sand fly–derived *Leishmania* promastigotes, PLoS Neglected Trop. Dis. 13 (2019), e0007288, https://doi.org/10.1371/journal.pntd.0007288.
[42] E. Torreira, S. Jha, J.R. López-Blanco, E. Arias-Palomo, P. Chacón, C. Cañas, S. Ayora, A. Dutta, O. Llorca, Architecture of the pontin/reptin complex, essential in the assembly of several macromolecular complexes, Structure 16 (2008) 1511–1520, https://doi.org/10.1016/j.str.2008.08.009.
[43] A. Jeganathan, V. Leong, L. Zhao, J. Huen, N. Nano, W.A. Houry, J. Ortega, Yeast Rvb1 and Rvb2 proteins oligomerize as a conformationally variable dodecamer with low frequency, J. Mol. Biol. 427 (2015) 1875–1886, https://doi.org/10.1016/j.jmb.2015.01.010.
[44] K.L.Y. Cheung, J. Huen, W.A. Houry, J. Ortega, Comparison of the multiple oligomeric structures observed for the Rvb1 and Rvb2 proteins, Biochem. Cell. Biol. 88 (2010) 77–88, https://doi.org/10.1139/o09-159.
[45] Y.J. Chen, X. Yu, E.H. Egelman, The hexameric ring structure of the *Escherichia coli* RuvB branch migration protein, J. Mol. Biol. 319 (2002) 587–591, https://doi.org/10.1016/S0022-2836(02)00353-4.
[46] M. Petukhov, A. Dagkessamanskaja, M. Bommer, T. Barrett, I. Tsaneva, A. Yakimov, R. Quéval, A. Shvetsov, M. Khodorkovskiy, E. Käs, M. Grigoriev, Large-scale conformational flexibility determines the properties of AAA+ TIP49 ATPases, Structure 20 (2012) 1321–1331, https://doi.org/10.1016/j.str.2012.05.012.
[47] K.L.Y. Cheung, J. Huen, Y. Kakihara, W.A. Houry, J. Ortega, Alternative oligomeric states of the yeast Rvb1/Rvb2 complex induced by histidine tags, J. Mol. Biol. 404 (2010) 478–492, https://doi.org/10.1016/j.jmb.2010.10.003.
[48] A. Niewiarowski, A.S. Bradley, J. Gor, A.R. McKay, S.J. Perkins, I.R. Tsaneva, Oligomeric assembly and interactions within the human RuvB-like RuvBL1 and RuvBL2 complexes, Biochem. J. 429 (2010) 113–125, https://doi.org/10.1042/BJ20100489.
[49] J.C. Borges, C.H.I. Ramos, Analysis of molecular targets of *Mycobacterium tuberculosis* by analytical ultracentrifugation, Curr. Med. Chem. 18 (2011) 1276–1285.
[50] S. Jha, A. Dutta, RVB1/RVB2: running rings around molecular biology, Mol. Cell 34 (2009) 521–533, https://doi.org/10.1016/j.molcel.2009.05.016.
[51] M.J. Davey, C. Indiani, M. O'donnell, Reconstitution of the Mcm 2-7p heterohexamer, subunit arrangement, and ATP site architecture, J. Biol. Chem. 278 (2003) 4491–4499, https://doi.org/10.1074/jbc.M210511200.